

## Large-Scale Effects on the Regulation of Tropical Sea Surface Temperature

DENNIS L. HARTMANN AND MARC L. MICHELSEN

*Department of Atmospheric Sciences, University of Washington, Seattle, Washington*

(Manuscript received 21 August 1992, in final form 21 January 1993)

### ABSTRACT

The dominant terms in the surface energy budget of the tropical oceans are absorption of solar radiation and evaporative cooling. If it is assumed that relative humidity in the boundary layer remains constant, evaporative cooling will increase rapidly with sea surface temperature (SST) because of the strong temperature dependence of saturation water vapor pressure. The resulting stabilization of SST provided by evaporative cooling is sufficient to overcome positive feedback contributed by the decrease of surface net longwave cooling with increasing SST. Evaporative cooling is sensitive to small changes in boundary-layer relative humidity. Large and negative shortwave cloud forcing in the regions of highest SST are supported by the moisture convergence associated with large-scale circulations. In the descending portions of these circulations the shortwave cloud forcing is suppressed. When the effect of these circulations is taken into account by spatial averaging, the area-averaged cloud forcing shows no sensitivity to area-averaged SST changes associated with the 1987 warming event in the tropical Pacific. While the shortwave cloud forcing is large and important in the convective regions, the importance of its role in regulating the average temperature of the tropics and in modulating temperature gradients within the tropics is less clear. A heuristic model of SST is used to illustrate the possible role of large-scale atmospheric circulations on SST in the tropics and the coupling between SST gradients and mean tropical SST. The intensity of large-scale circulations responds sensitively to SST gradients and affects the mean tropical SST by supplying dry air to the planetary boundary layer. Large SST gradients generate vigorous circulations that increase evaporation and reduce the mean SST.

### 1. Introduction

Geological evidence suggests that average tropical sea surface temperatures have not varied by more than a few degrees Celsius, while polar temperatures have undergone variations of more than ten degrees (CLIMAP 1981; Rind and Petzet 1985; Manabe and Broccoli 1985). Global climate models (GCMs) show a similar polar amplification of surface temperature changes in response to a wide variety of climate forcings (e.g., Manabe and Wetherald 1980; Hansen et al. 1984; Hansen et al. 1988; Washington and Meehl 1984). This so-called polar amplification is often attributed to polar processes such as surface ice cover and low-level static stability that increase the sensitivity of the surface temperature in polar latitudes. It is also true that the polar amplification of climate change is in part a result of tropical processes that make tropical surface temperature relatively stable.

The insensitivity of tropical surface temperatures is directly related to the sensitivity of saturation water vapor pressure to temperature (Sarachik 1978). The vapor pressure affects many processes of importance for the surface energy balance in the tropics. Water

vapor is the principal greenhouse gas, and in the tropics as the temperature increases the downward emission of longwave radiation increases more rapidly than the upward emission from the surface, so that the longwave cooling of the surface decreases. This strong greenhouse effect is of course a positive feedback that acts to make the tropical SST more sensitive. This positive feedback can be offset by evaporative cooling of the tropical sea surface, which may increase more rapidly with SST than the longwave cooling is reduced. The climatological relative humidity of the atmospheric boundary layer over the tropical oceans remains in a narrow range around 80%, whether in the trade-wind or ITCZ regions (Fitzjarrald and Garstang 1981), though day-to-day variations with a standard deviation of 10%–15% are associated with meteorological activity. Because of the rapid increase of saturation vapor pressure with temperature, fixed relative humidity would imply that the evaporation increases rapidly with SST, all else being equal. The increase of evaporation with temperature under these conditions constitutes a very strong negative feedback on SST.

Because the specific humidity of surface air increases rapidly with surface temperature, the moist static energy of surface air also increases rapidly with temperature. If the temperature and humidity profiles above the boundary layer do not change radically, the increased surface moist static energy implies more intense

---

*Corresponding author address:* Dr. Dennis L. Hartmann, Department of Atmospheric Sciences, AK-40, University of Washington, Seattle, WA 98195.

convection, which might maintain buoyancy to a higher altitude, at least until the tropospheric temperature distribution adjusts to the enhanced convective heating. The effects of this more intense convection are complex and important. More intense convection will be associated with more rainfall, which means that more energy will be removed from the tropical boundary layer, primarily by drying, but also through evaporatively driven cold downdrafts (Houze and Betts 1981). Drying and cooling of the boundary layer by the mesoscale wind circulations associated with convection will facilitate further cooling of the surface (Fitzjarrald and Garstang 1981). Through latent heat release and longwave trapping, the convection will also provide substantial mean heating to the atmosphere locally, which will be balanced by adiabatic expansion associated with large-scale rising motion. This large-scale rising motion in the region of convection must be balanced by large-scale subsidence elsewhere. Most of this subsidence occurs over the warm tropical waters adjacent to the convective region. The entrainment of this dry subsiding air into the planetary boundary layer supports evaporation in the trade-wind region. The water evaporated in the trade winds is carried in the atmosphere to the convective regions where it supports the development of intense convection. The cooling and drying of the atmospheric boundary layer, which drives the evaporative cooling of the ocean surface, is thus a cooperative venture between the mesoscale and large-scale circulations in the tropical atmosphere.

It is uncertain which processes provide the dominant mechanism for making tropical surface temperatures relatively stable through geologic time. Ramanathan and Collins (1991, hereafter RC) argue that the dominant mechanism for constraining SST in the regions of warmest water temperature must be the reduction of absorbed solar energy that is caused by the development of convective clouds and their associated anvils, which have high albedos. The importance of shortwave cloud feedback was inferred by estimating the sensitivity of shortwave cloud forcing to SST in two ways. First the spatial gradients of SST and shortwave cloud forcing were compared and a regression relationship between temperature and shortwave cloud forcing developed therefrom. Second, the local SST and shortwave cloud forcing changes associated with an El Niño–Southern Oscillation (ENSO) warm event were compared. In both cases a strong sensitivity of shortwave cloud forcing to SST of about  $-25 \text{ W m}^{-2} \text{ K}^{-1}$  was inferred. This estimate is much larger than any other likely sensitivity of a surface energy flux term to SST, and would imply a very stable surface temperature if it were an accurate measure of the response of cloud albedo to SST. In both of the estimates RC attribute the cloud albedo changes to the SST, whereas much of the shift in cloud properties between the warm and warmest regions of the tropics is associated with the large-scale atmospheric circulations that

accompany the SST gradients, and not with the absolute value of the SST itself.

In this paper the evidence for cloud feedback provided by RC is evaluated in light of the strong coupling between convective and large-scale processes described above. While the dependence of cloud albedo on temperature may appear very large when evaluated locally, the effect is small when averaged over the domain occupied by the large-scale circulation that supports the intense convection over the warmest water. The large-scale circulation both supports intense convection and high albedos where it is converging at low levels and suppresses cloudiness and cloud albedo where it is diverging. These two effects appear to cancel out in the case of the 1987 warm event in the Pacific, so that the area-averaged cloud forcing shows no apparent sensitivity to area-averaged SST. It is possible that the cloud shortwave feedback strongly damps spatial gradients of SST within the tropics. However, as Wallace (1992) has argued, dynamical processes also work very efficiently to maintain weak temperature gradients within the tropics, and convection in the region of warmest water “feels” the temperature of the entire tropical troposphere because of this efficient communication in the free troposphere.

We can estimate the terms in the surface energy balance and their sensitivity to SST changes. We note that solar heating and evaporative cooling are the largest terms. Using the aerodynamic formula for evaporation as a guide, it is evident that evaporative cooling is very sensitive to SST, relative humidity in the atmospheric boundary layer, and the intensity of turbulence in the atmospheric boundary layer. If we assume that the relative humidity is insensitive to time- and area-averaged SST, the aerodynamic formula implies a substantial sensitivity of evaporative cooling to SST, which is adequate to overcome the positive feedback provided by the water vapor greenhouse effect and yield a very stable tropical SST.

To illustrate the potential role of large-scale dynamics in connecting SST gradients with mean SST, we construct a very simple heuristic model of the surface energy balance that includes spatial communication through the atmospheric boundary layer and the effect of the large-scale atmospheric circulations on the energy balance of the ocean. This model provides the provocative result that the effect of shortwave cloud forcing in damping SST gradients may actually result in a net increase of the average SST of the tropics. This result is based on the assumption that the large-scale circulation can decrease the relative humidity in the boundary layer by subsidence drying in regions of low-level divergence, but large-scale convergence cannot increase the relative humidity above the level at which convection will be initiated. Therefore, any process that damps SST gradients in the tropics will reduce the ventilation of the boundary layer by the circulation and thereby reduce the evaporation rate.

## 2. Surface energy budget

The energy balance of the surface mixed layer of the tropical oceans can be written schematically as follows:

$$c \frac{\partial T_s}{\partial t} = SW + LW - LE - SH - \Delta F_o = H, \quad (1)$$

where  $T_s$  is both the temperature of the oceanic mixed layer and the SST,  $c$  the heat capacity of the mixed layer,  $SW$  and  $LW$  are the net solar and longwave radiative heating of the surface, respectively,  $LE$  and  $SH$  are the latent and sensible turbulent heat fluxes away from the surface,  $\Delta F_o$  is the export of heat out of the region by oceanic transport, and  $H$  is the net energy balance of the mixed layer. Under current conditions the long-term mean energy content of the tropical oceanic mixed layer is approximately constant, and the five energy flux terms in (1) add up to zero. The main drive is of course solar heating of the surface, which is roughly  $200 \text{ W m}^{-2}$  when averaged over the region from  $30^\circ\text{S}$  to  $30^\circ\text{N}$ . This is balanced by cooling from evaporation ( $\sim 120 \text{ W m}^{-2}$ ), longwave cooling ( $\sim -50 \text{ W m}^{-2}$ ), sensible heat flux ( $\sim 10 \text{ W m}^{-2}$ ), and meridional energy transport in the ocean ( $\sim 20 \text{ W m}^{-2}$ ) (e.g., Oberhüber 1988; Sellers 1965). To investigate how this surface energy balance might respond to a temperature perturbation induced by an externally imposed energy balance change, we will perform a rough sensitivity analysis by introducing simple representations for each of the terms in the surface energy balance (1).

### a. Longwave cooling of the surface

One might think naively that net longwave cooling of the surface would increase with temperature because of the Planck function dependence on temperature, but the net longwave loss actually gets smaller with increasing temperature (Ramanathan 1981), and especially rapidly for tropical conditions. This is because of the strong dependence of saturation water vapor pressure on temperature and the strong dependence of continuum absorption on the partial pressure of water vapor. For example, we consider clear-sky conditions, and assume that the lapse rate and relative humidity remain constant as the surface temperature is varied. Figure 1 shows the net longwave heating of the surface as a function of temperature calculated with the radiative transfer model of Wiscombe and Evans (1977).<sup>1</sup> This model uses the parameterization of water vapor continuum absorption proposed by Roberts et al. (1976). The total flux is shown along with the flux in the water vapor window region ( $8\text{--}12 \mu\text{m}$ ) and the ro-

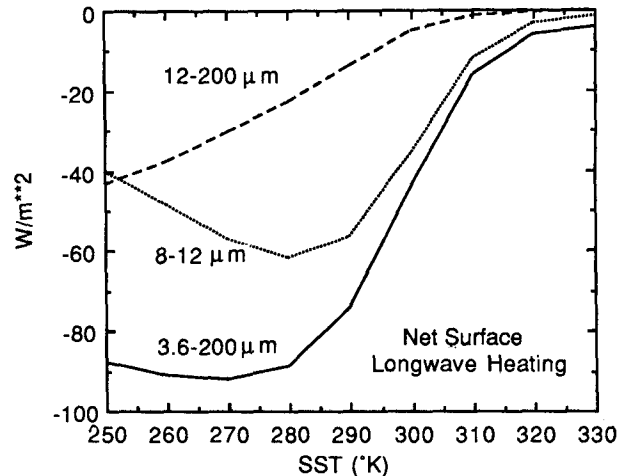


FIG. 1. Net longwave heating of the surface in  $\text{W m}^{-2}$  as a function of SST calculated using a radiative transfer model with fixed relative humidity and lapse rate. Curves are shown for fluxes from various wavelength ranges:  $12\text{--}200 \mu\text{m}$ ,  $8\text{--}12 \mu\text{m}$ , and  $3.6\text{--}200 \mu\text{m}$ .

tation bands of water vapor ( $12\text{--}200 \mu\text{m}$ ). At temperatures below about  $280 \text{ K}$  the net longwave loss increases with temperature because of the dependence of surface emission on temperature. At temperatures above  $280 \text{ K}$  the net longwave loss from the surface begins to decrease rapidly with increasing temperature, because of the rapid closure of the water vapor window in the  $8\text{--}12\text{-}\mu\text{m}$  region by continuum absorption (Hallberg and Inamdar 1993). These numbers were derived for a lapse rate of  $6.5 \text{ K km}^{-1}$ , a constant minimum temperature of  $200 \text{ K}$  in the stratosphere, and the relative humidity profile used by Manabe and Wetherald (1967).

The basic structure of Fig. 1 is insensitive to the use of different lapse rates, relative humidity profiles, or assuming a moist-adiabatic lapse rate above the surface. The behavior exhibited depends critically on the temperature dependence of specific humidity in the planetary boundary layer, which is strongly dependent on surface temperature. Varying the relative humidity within the range of  $70\%$  to  $90\%$  has only a weak effect on the location of the rapid cutoff in the vicinity of  $300 \text{ K}$ . Outgoing longwave radiation is much more sensitive to lapse rate and upper-tropospheric relative humidity than is the surface net longwave radiation. The effect of adding fixed cloudiness would be to decrease the rate at which the longwave cooling decreases with temperature, because cloud would reduce the longwave cooling at the lower temperatures but would have little effect at the highest temperatures, where the cloud-free boundary layer is already virtually opaque to longwave radiation.

The dependence of surface longwave cooling on surface temperature depicted in Fig. 1 constitutes a positive feedback at the temperatures of the tropical sea surface, since as the temperature increases the longwave

<sup>1</sup> The code we used is called "atrad" and is familiar to many people. Its longwave fluxes fall near the middle in an intercomparison of many models (Ellingson et al. 1991).

cooling is reduced. According to these calculations, near 300 K the longwave heating of the surface increases with surface temperature at a rate of about  $2.8 \text{ W m}^{-2} \text{ K}^{-1}$ . Although the blackbody emission of the surface increases with temperature of the surface at the rate of about  $6 \text{ W m}^{-2} \text{ K}^{-1}$ , the downward longwave emission at the surface increases more rapidly at a rate of about  $9 \text{ W m}^{-2} \text{ K}^{-1}$ . If tropical SST is truly stable, then other mechanisms must overcome the sensitivity contributed by the water vapor greenhouse feedback.

### b. Solar heating of the surface<sup>2</sup>

If the net insolation at the surface is sensitive to surface temperature, then clouds are the most likely cause. Cloud physics may be sensitive to temperature in such a way as to constitute a negative feedback (e.g., Somerville and Remer 1984; Roeckner et al. 1987; Mitchell et al. 1989). Biological processes in the ocean and their link with cloud radiative properties may also constitute a feedback process (Charlson et al. 1987). These feedbacks are potentially important, but convincing demonstrations of their real effects on temperature sensitivity in general, and on the tropical SST in particular, have yet to be given.

RC used the correspondence between high SST and high cloud albedos associated with convective anvil clouds to argue that cloud albedo constitutes a powerful negative feedback that constrains tropical SST below a critical value of about 303 K. They evaluate the sensitivity of the shortwave cloud forcing to SST by looking at the spatial relationship between these two quantities and the changes in this spatial relationship that occur between El Niño and non-El Niño years. In both cases they infer that a 1-K increase in SST is accompanied by about a  $25\text{-W m}^{-2}$  cloud-induced decrease in surface insolation, which would imply an extremely potent negative cloud shortwave feedback on surface temperature.

One can ask, however, what fraction of the enhancement of cloud albedo over the warmest water is associated with the absolute value of the temperature, and what fraction is associated with the temperature gradients and the large-scale circulations that these temperature gradients induce. Our concern is illustrated in Fig. 2, which shows the shortwave cloud forcing and the total atmospheric greenhouse effect at the top of the atmosphere estimated from ERBE data (Barkstrom 1984; Ramanathan et al. 1989) plotted versus SST in the tropical Pacific Ocean between  $20^{\circ}\text{S}$  and  $20^{\circ}\text{N}$  (Reynolds 1988) and versus the large-scale divergence at 200 mb calculated from European Centre for Medium-Range Weather Forecasts (ECMWF) analyses

for the March–May season during 1987. Each point represents one  $2.5^{\circ} \times 2.5^{\circ}$  region. When plotted versus SST the shortwave cloud forcing and greenhouse effect are not linearly related to the SST. Apparently, some other important factor is needed to explain the abrupt change in the relationships within the tropics.

The “hooklike” structure in Figs. 2a and 2c is associated with the Hadley and Walker circulations, which support intense convection where they converge at low levels and suppress cloudiness where they diverge. Between about 301 K and the warmest temperature of about 303 K, the shortwave cloud forcing is equally likely to fall anywhere in the range of  $-10$  to  $-100 \text{ W m}^{-2}$ . It is more reasonable to suppose that the shortwave cloud forcing is independent of SST in this region than it is to assume a steeply sloping linear dependence, since a linear fit explains a small fraction of the variance for the region from  $20^{\circ}\text{S}$  to  $20^{\circ}\text{N}$ .

As shown in Figs. 2b and 2d, the shortwave cloud forcing and the total greenhouse effect are linearly related to the divergence at 200 mb (with substantial scatter). The vertical velocity at 500 mb and the convergence at 850 mb are both linearly related to the 200-mb divergence for most tropical motions and produce similar plots. The largest greenhouse and shortwave forcings all occur where the large-scale flow is converging at low levels. The convective clouds and the large-scale vertical motion field are inextricably linked. A convergence of moisture by the large-scale circulation is required to drive the intense convection that produces the bright anvil clouds in the tropics (Cornejo-Garrido and Stone 1977). The heating by latent heat release and longwave radiation in the convective clouds is in turn required to drive the large-scale vertical motion (e.g., Holton 1992).

One can see that the regions of enhanced convective cloud are linked with regions of suppressed convective cloud by mapping the changes in shortwave cloud forcing from a year with cool Pacific SST (1985) to a warm event year (1987). Figure 3 shows the difference in the shortwave cloud forcing between 1987 and 1985 for the March through May (MAM) season. This season is chosen because it has the warmest SST in the central and eastern Pacific Ocean. Other seasons show similar behavior. Note the large region with enhanced cloud shortwave cooling of up to  $-60 \text{ W m}^{-2}$  along the equator in the central and eastern Pacific Ocean where the warm SST anomalies occur. Note also, however, that the region of enhanced cloud shortwave cooling is flanked by changes of opposite sign, which reach  $+40 \text{ W m}^{-2}$  in places and extend over a larger area than the region of enhanced cloud shortwave cooling.

The regions with compensating changes in shortwave cloud forcing are connected to each other by the large-scale circulation that joins the region of intense tropical convection to the rest of the tropics. Intense tropical convection is associated with heating of the atmo-

<sup>2</sup> The work described in this section was first presented at the symposium on “Aerosol–Cloud–Climate Interactions” held at the XX Assembly of the International Union of Geodesy and Geophysics, Vienna, Austria, 13–20 August 1991.

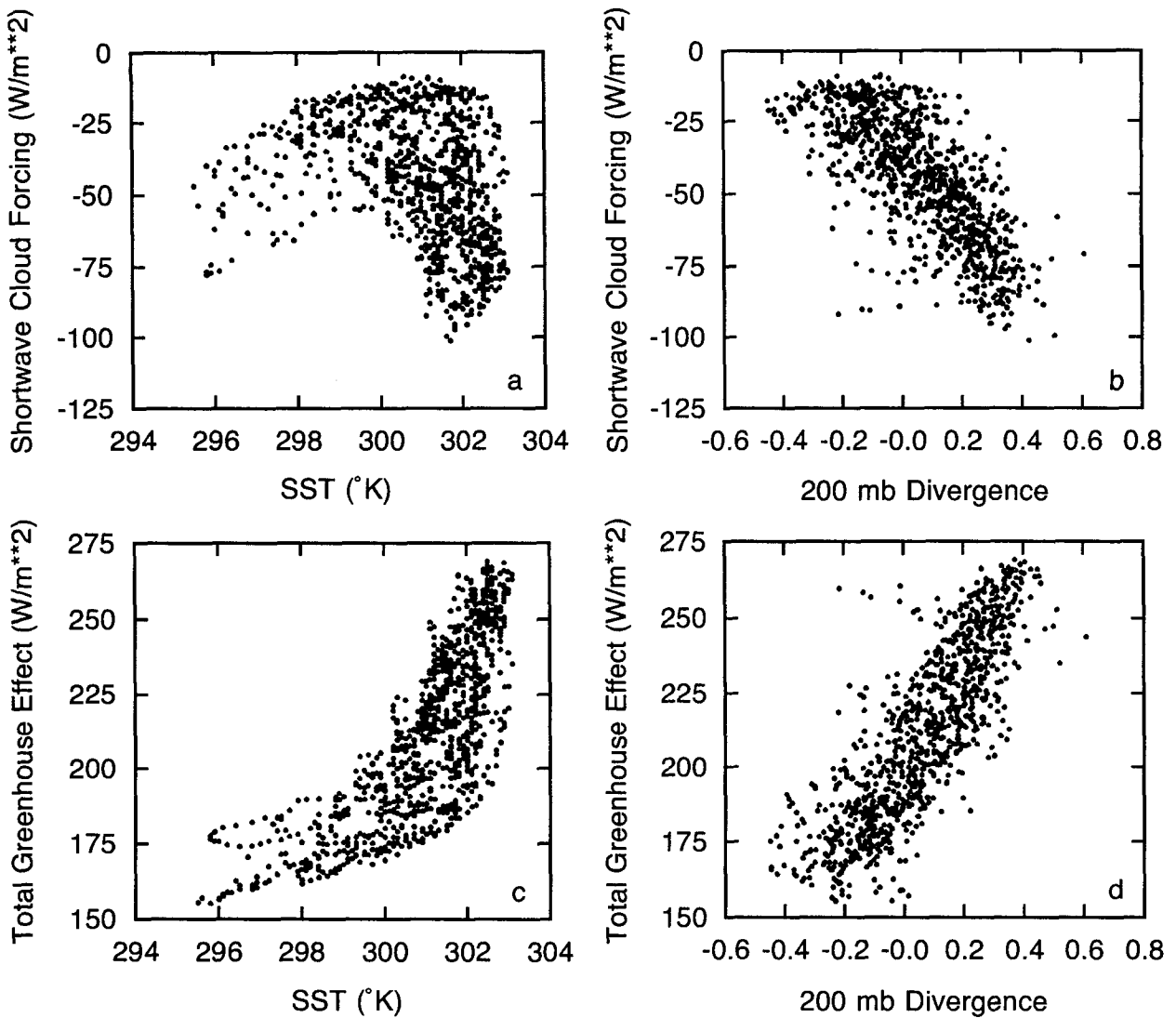


FIG. 2. Scatter diagrams of (a) shortwave cloud forcing ( $C_s$ ) and (c) total greenhouse effect ( $G$ ) versus SST, and (b) shortwave cloud forcing and (d) total greenhouse effect versus divergence at 200 mb.

sphere, which drives large-scale upward motion. This net upward motion in the convective region must be compensated by net downward motion in some other region to satisfy the requirements of mass balance. The majority of this compensating downward motion also occurs in the tropics, often in the near vicinity of the convective region, where the SST is not very different from that in the region of ascent. The subsidence suppresses cloudiness and cloud albedo above and within the boundary layer. The proximity of convectively driven large-scale ascent and its compensating large-scale subsidence is part of the explanation for the fact that almost cloudless skies occur in near proximity and at virtually the same SST as skies that are congested with intense mesoscale convective systems and their associated anvil

clouds. This, in turn, is related to the fact that very strong and very weak shortwave cloud forcing tend to exist within a narrow range of temperatures near the maximum values observed (Fig. 2a). We therefore conclude that the steep increase in convective cloud forcing of albedo and longwave emission near the highest temperatures that occur in the tropics is related in large part to the influence of the large-scale circulation on the convection. The location and intensity of these circulations are strongly influenced by SST gradients and dynamical constraints as well as to the absolute value of SST. Fu et al. (1992) have argued that the properties of the convective anvil and cirrus clouds do not respond sensitively to SST, and have also pointed out the important role of large-scale circulations.

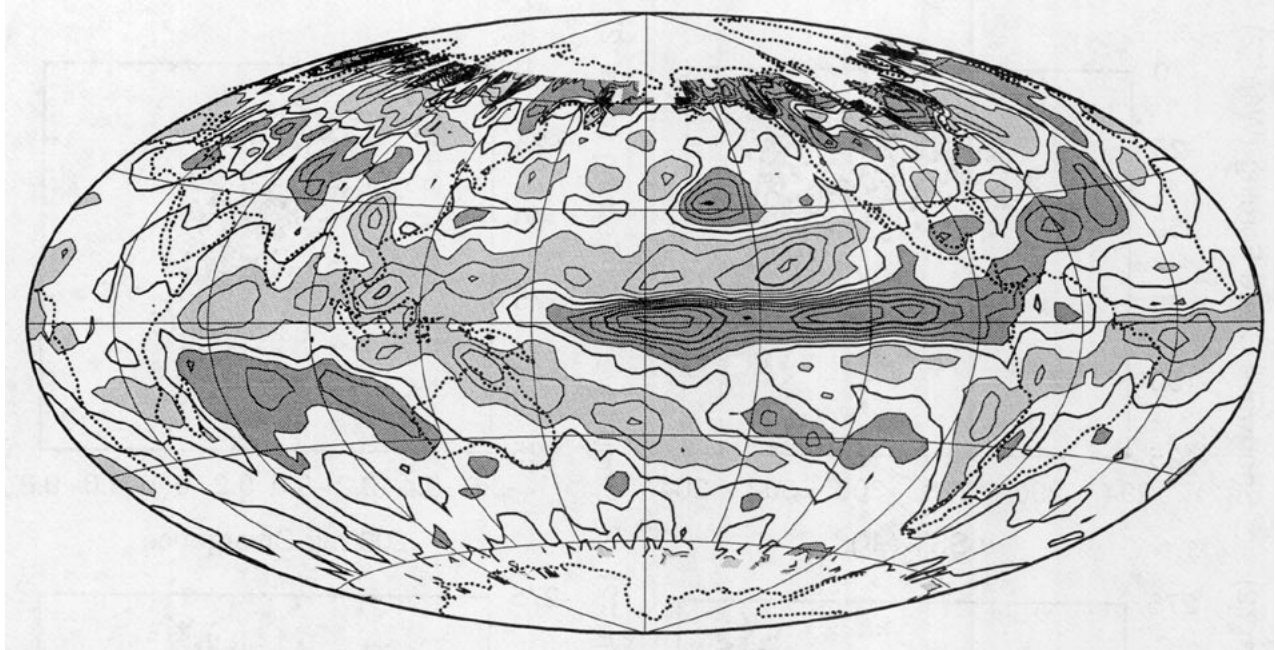


FIG. 3. Map of the difference in shortwave cloud forcing between MAM 1987 and MAM 1985. Contour interval is  $10 \text{ W m}^{-2}$ . Values larger than  $10 \text{ W m}^{-2}$  are lightly shaded and values less than  $-10 \text{ W m}^{-2}$  are heavily shaded.

To attempt an estimate of the effect of shortwave cloud forcing on the sensitivity of tropical SST, one can compute the changes of SST and shortwave cloud forcing averaged over an area that includes the large-scale atmospheric circulation associated with the convective heating. Figure 3 suggests using a region that is comparable in scale to the Hadley circulation, as one would expect, so that an average over the tropical belt from  $30^\circ\text{S}$  to  $30^\circ\text{N}$  is implied. The east–west Walker circulation also responds to the anomalous convective heating, so that averaging across a broad range of longitudes is appropriate. Table 1 shows the sensitivity to SST of various energy balance components that is implied by dividing changes in energy balance quantities between MAM 1987 and 1985 by the SST difference between these two seasons. The first column shows the SST sensitivity implied by an average over the region of greatest shortwave cloud forcing change, where the average temperature warms by 1.9 K. The resulting sensitivity is similar to the values that would be obtained by considering a single point in this region. The net radiation at the top of the atmosphere does not change significantly, but the absorbed solar radiation decreases by  $-21 \text{ W m}^{-2} \text{ K}^{-1}$  and the outgoing longwave radiation (OLR) decreases by a similar amount. The nearly perfect compensation of shortwave and longwave fluxes at the top of the atmosphere associated with tropical cloud changes is commonly observed, but why such close compensation should occur is not fully understood. This compensation at the top of the atmosphere is maintained for averages over a larger spatial domain, but the individual contributions from

shortwave and longwave cloud forcing both decrease as the area of averaging is increased to include both the convective regions and the associated regions of large-scale subsidence. By the time one has averaged over the region in the Pacific Ocean from  $20^\circ\text{S}$  to  $20^\circ\text{N}$ , the estimated sensitivity of shortwave cloud forcing to SST has decreased to essentially zero, while the SST change averaged over this region is still a substantial  $0.6^\circ\text{C}$ . The estimated sensitivity of the greenhouse effect to SST also decreases with the size of the averaging area, but not as quickly or completely as that of the shortwave cloud forcing, so that a substantial positive greenhouse feedback is inferred even for averages over large areas (see also Raval and Ramanathan 1989; Stephens and Greenwald 1991). This is presumably because the lower-tropospheric water vapor content is closely tied to the SST and does not respond as strongly to the large-scale circulation as the convective cloud and the upper-tropospheric water vapor.

The results in Table 1 and Figs. 2 and 3 suggest that the shortwave cloud forcing responds locally to the convergence or divergence of the large-scale flow field, and that there is relatively little evidence that the average tropical cloud albedo responds strongly to average SST. If one asserts that the large-scale circulation responds sensitively to SST gradients in the tropics (e.g., Lindzen and Nigam 1987, hereafter LN), then one may conclude that the local shortwave cloud forcing is more sensitive to SST gradients than to the absolute value of SST. For example, if the SST were uniformly raised by  $1^\circ\text{C}$  at every point, the cloud shortwave cooling would not increase everywhere in proportion to the

TABLE 1. Estimates of the sensitivity of radiative energy balance components to sea surface temperature ( $T_s$ ) obtained by differencing March through May seasonal averages from 1985 and 1987 over ocean areas within the geographical regions indicated. The "Pacific" is defined as the ocean areas falling within the longitude range of 120°E to 70°W. The first row gives the area-averaged SST difference between the two years in °C. The remaining rows give the quantities indicated in  $Wm^{-2} K^{-1}$ . Subscript CS indicates a clear-sky value.  $OLR$  = outgoing longwave radiation at the top of the atmosphere,  $G$  = total greenhouse effect of atmosphere =  $\sigma T_s^4 - OLR$ ,  $G_a$  = clear atmosphere greenhouse effect =  $\sigma T_s^4 - OLR_{CS}$ ,  $C_l$  = longwave forcing by clouds =  $OLR_{CS} - OLR$ ,  $Q$  = absorbed solar radiation,  $C_s$  = shortwave cloud forcing =  $Q_{CS} - Q$ ,  $R^\infty$  = net radiation at the top of the atmosphere.

	5°N-5°S 180-90°W	10°N-10°S Pacific	20°N-20°S Pacific	30°N-30°S Pacific
$\Delta T_s$	1.9	0.9	0.6	0.4
$4\sigma T_s^3$	6.2	6.2	6.1	6.1
$dOLR$				
$\frac{dT_s}{dOLR_{CS}}$	-20.5	-12.5	-0.7	2.8
$\frac{dG}{dT_s}$	-2.6	-1.0	1.6	1.8
$\frac{dG_a}{dT_s}$	26.7	18.6	6.9	3.3
$\frac{dC_l}{dT_s}$	8.7	7.1	4.6	4.3
$\frac{dQ}{dT_s}$	18.0	11.5	2.3	-1.0
$\frac{dQ_{CS}}{dT_s}$	-21.0	-12.1	-0.7	1.9
$\frac{dC_s}{dT_s}$	0.6	0.4	0.1	0.4
$\frac{dR^\infty}{dT_s}$	-21.6	-12.5	-0.8	1.1
$\frac{dR_{CS}^\infty}{dT_s}$	-0.5	0.3	0.0	-0.9
$\frac{dC_l + dC_s}{dT_s}$	3.1	1.4	-1.5	-1.4
$\frac{dC_l}{dT_s} + \frac{dC_s}{dT_s}$	-3.7	-1.0	1.5	0.6

changes observed in going from the cold SST region to the warm SST region in the current climate. The results in Table 1 suggest that the best estimate would be that no changes in average cloud shortwave cooling would result from a uniform increase in SST. This constitutes the null hypothesis that needs to be disproved in order to infer a large role for cloud albedo feedback in climate sensitivity.

Though there is little in the evidence presented here to conclude that the effect of convective clouds on surface insolation constitutes a strong feedback on the average SST of the tropics, it may be that they help to sustain the relatively uniform SST in the warmest regions. Because highly reflective clouds occur in the region of low-level convergence that tends to form over the warmest SST, it is possible that the effect of clouds on absorbed solar radiation helps to maintain weak

temperature gradients and relatively uniform SST over the tropical oceans. There are, of course, large-scale influences that would also tend to make the SST gradients in the tropics weak (Wallace 1992). In section 3 we will employ a simple model to investigate the role of SST gradients in the heat balance of the tropical oceans.

c. Evaporation cooling

According to the bulk aerodynamic formulation (Arya 1988), evaporative cooling of the surface can be expressed as a linear function of the specific humidity contrast between the air in contact with the surface  $q_s$ , and the air at some distance above the surface  $q_a$ , usually taken to be 10 m, but characterizing the bulk of the boundary-layer air that is in efficient communication with the surface:

$$LE = L\rho_a C_D U (q_s - q_a). \tag{2}$$

We will use (2) to make an estimate of the sensitivity of evaporative cooling to SST. The air in contact with the ocean surface is usually taken to be saturated, so that  $q_s = q_s^*$ . The specific humidity of the air in the boundary layer can be approximated in terms of its relative humidity (RH), and the surface saturation mixing ratio:

$$q_a = RH \left( q_s^* + \frac{\partial q^*}{\partial T} (T_a - T_s) + \dots \right) \approx RH q_s^*. \tag{3}$$

We thus can write an approximation to (2) that contains the saturation specific humidity and the relative humidity of the air as parameters:

$$LE \approx L\rho_a C_D U q_s^* (1 - RH). \tag{4}$$

In evaluating the sensitivity of (4) to SST we will assume that the product of air density, drag coefficient, and wind speed is a fixed constant. This is the simplest assumption, and there is little justification for assuming anything else, since it is hard to anticipate how these might change with mean SST. This leaves the saturation mixing ratio and the relative humidity as the key variables. Since we have no basis for postulating anything more complicated, we will assume that the relative humidity remains constant as the mean temperature of the tropics changes. Under these conditions it is only the saturation mixing ratio that changes with temperature, and it can be shown from (4) and the Clausius-Clapeyron relation that

$$\frac{1}{LE} \frac{\partial LE}{\partial T_s} \approx \frac{L}{R_v T_s^2} \approx 6 \times 10^{-2} K^{-1} \tag{5}$$

where  $L$  is the latent heat of vaporization,  $R_v$  is the gas constant for water vapor, and the numerical value is obtained for a temperature of 300 K. If  $LE = 120 W m^{-2}$ , we have that

$$\left. \frac{\partial LE}{\partial T_s} \right)_{RH=\text{const.}} \approx 7.2 \text{ W m}^{-2} \text{ K}^{-1}. \quad (6)$$

For fixed exchange coefficient and relative humidity, the dependence of evaporative cooling on surface temperature is strongly stabilizing, and this estimate would indicate that it is large enough in magnitude to overcome the destabilizing effect of surface longwave cooling. Sensible cooling of the surface is relatively unimportant in the tropics compared to latent cooling, and we will ignore its possible sensitivity to mean temperature.

One must note, however, that the evaporative cooling (4) is extremely sensitive to the relative humidity. From (4) we can infer that for fixed temperature, each percent increase in relative humidity will decrease the evaporative cooling by about  $8 \text{ W m}^{-2}$  (if  $LE = 120 \text{ W m}^{-2}$  and  $RH = 85\%$ ):

$$\left. \frac{\partial LE}{\partial RH} \right)_{q^*=\text{const.}} \approx \frac{-LE}{(1-RH)} \approx -8 \text{ W m}^{-2} \%^{-1}. \quad (7)$$

This underscores the great importance of understanding and predicting the thermodynamic properties of the tropical atmospheric boundary layer and their relationship with the mean climate and circulation.

#### d. Overall sensitivity

Based on the analysis of this section, we would assume that the shortwave cloud forcing is independent of mean SST, but that net longwave heating of the surface increases with temperature. For the evaporative cooling we hypothesize that the relative humidity will remain constant as the temperature changes. It cannot be proven that the relative humidity will remain constant, but this assumption is often invoked in climate sensitivity analysis and has proven to be an excellent first approximation in the case of one-dimensional radiative modeling. We ignore for now the effect of changing horizontal energy transport by the ocean, so that our estimate of the overall sensitivity of the surface energy balance to surface temperature is moderately large and negative:

$$\begin{aligned} \frac{\partial H}{\partial T_s} = \frac{\partial SW}{\partial T_s} + \frac{\partial LW}{\partial T_s} - \frac{\partial LE}{\partial T_s} - \frac{\partial SH}{\partial T_s} - \frac{\partial \Delta F_o}{\partial T_s} \approx 0 \\ + 2.8 - 7.2 - 0 - ? \approx -4.4 \text{ W m}^{-2} \text{ K}^{-1}. \quad (8) \end{aligned}$$

These assumptions yield a sensitivity to external forcing of  $0.23 \text{ K}$  change in temperature for a  $1 \text{ W m}^{-2}$  forcing. This implies a relatively insensitive surface climate and relatively stable SST, which can be attributed to the evaporative feedback. Sensitivity experiments with global climate models also suggest that among the surface energy balance components, latent cooling responds most to changes in surface temperature and overcomes changes of opposite sign in the net longwave flux (Randall et al. 1992).

### 3. A heuristic model with SST gradients

Any discussion of SST gradients in the tropics must include the very substantial influence of these gradients on the large-scale circulation of the tropics. The large-scale circulation affects the SST by ventilating the atmospheric boundary layer, moving water vapor laterally, and driving ocean currents. We present here a simple model of the coupled atmosphere–ocean system whose purpose is to illustrate how SST gradients might interact with large-scale atmospheric circulation patterns to modulate both SST gradients and mean SST. The model focuses on the role of the moisture budget of the tropical atmospheric boundary layer.

The model includes the surface energy balance (1) and an equation for the specific humidity of the atmospheric boundary layer. The oceanic heat transport is externally specified and does not interact with the atmospheric circulation. For simplicity, we formulate the model in one horizontal dimension, so that the specific humidity evolution is described by the following equation:

$$\frac{\partial q}{\partial t} = -\frac{\partial}{\partial x}(uq) - \frac{\partial}{\partial z}(wq) + E - C. \quad (9)$$

Here  $q$  is the specific humidity,  $E$  is the evaporation rate, and  $C$  is the condensation rate. Humidity and horizontal velocity are assumed to be independent of height within the atmospheric boundary layer, which is assumed to be locally incompressible and to have a depth  $H_o = 3000 \text{ m}$ . The humidity in the atmosphere above the boundary layer is assumed to be zero. The wind in the boundary layer is calculated from the SST using the formulation proposed by LN. In their formulation, surface pressure perturbations are determined by the density variations within a tropical boundary layer of nearly constant depth, so that surface pressure is approximately inversely proportional to SST. It is assumed that convection acts to keep the boundary-layer depth almost constant, but a small adjustment time for the convection to achieve this balance gives rise to a “back pressure” correction, which gives some scale selection to the solution. All parameters required for the determination of  $u$  from  $T_s$  are as recommended by LN to produce the most realistic prediction of observed tropical surface winds from SST. Using equations (6), (7), and (10) from LN, an equation for the perturbation zonal velocity in one dimension can be derived, which can be written schematically as

$$\tau_c \frac{\partial^2 u'}{\partial x^2} + \frac{\tau_d^{-1}}{c_1} u' = \frac{c_2}{c_1} \frac{\partial T_s}{\partial x}, \quad (10)$$

where  $\tau_c$  is the adjustment time of the convective mass flux to the large-scale convergence (see LN),  $\tau_d$  is the linear relaxation time for surface drag, and  $c_1$  and  $c_2$  are constants. We see that the forcing for the zonal velocity is provided by the SST gradient, and some

suppression of small-scale responses is given by the provision of a nonzero  $\tau_c$ . We use  $\tau_c = 1800$  s. A uniform zonal wind of  $u_0 = 8 \text{ m s}^{-1}$  is added to the perturbation zonal wind determined from (10).

The energy balance of the ocean mixed layer is coupled to the atmospheric boundary layer through the evaporation rate. The evaporation rate is calculated using a bulk aerodynamic formula (2) whose coefficients are consistent with the linear drag law assumed in the boundary-layer wind parameterization. The linear relaxation time scale for both momentum and humidity is 2.5 days. Longwave cooling of the surface is parameterized in terms of the SST using an approximation to the solid curve in Fig. 1. Sensible cooling is ignored. To take account of the  $20 \text{ W m}^{-2}$  oceanic transport out of the tropics we assume that the insolation is  $180 \text{ W m}^{-2}$  rather than  $200 \text{ W m}^{-2}$ . If a relative humidity of 86% is assumed, then local energy balance gives an equilibrium temperature of 300.5 K, with an evaporative cooling rate of  $133 \text{ W m}^{-2}$  and a longwave loss of  $47 \text{ W m}^{-2}$ . This balance is in good agreement with the observed energy balance of the tropics, if we assume that the modeled evaporative cooling includes the sensible cooling. For fixed relative humidity the surface temperature is insensitive to insolation changes,

$$\frac{\partial T_s}{\partial SW} = 0.19 \text{ K (W m}^{-2}\text{)}^{-1} \quad (11)$$

because the evaporative cooling is relatively sensitive to the surface temperature,

$$\frac{\partial LE}{\partial T_s} = 7.9 \text{ W m}^{-2} \text{ K}^{-1}. \quad (12)$$

The sensitivity of the latent cooling to temperature (12) is in good agreement with our previous estimate (6). It is also important to note again the great sensitivity of the evaporation to the relative humidity in the boundary layer in this model (7). In terms of the surface temperature sensitivity to relative humidity, we have that

$$\frac{\partial T_s}{\partial RH} = 1.8 \text{ K}\%^{-1}. \quad (13)$$

If the aerodynamic formula can provide any kind of guidance, then the factors that determine relative humidity in the tropical boundary layer are of great importance.

We now consider the effect of SST gradients on the surface energy balance by calculating a joint solution to (1) and (9), using (10). We consider a model with an  $x$  dimension of 10 000 km, which we can think of as the equatorial Pacific. To generate an SST gradient we apply a sinusoidal energy exchange in  $x$ , which we can imagine represents the effect of ocean currents in driving a zonal gradient in SST:

$$\Delta F_o = D \sin\left(\frac{2\pi x}{d}\right); \quad (14)$$

$D$  is a magnitude in  $\text{W m}^{-2}$  and  $d$  is the length of the ocean basin.

Large-scale convergence in the boundary layer plus evaporation will quickly increase the relative humidity of the air in the boundary layer. In the atmosphere, increases of relative humidity above about 85% are not sustained for very long because cloud-scale motions are quick to utilize the latent energy of the humid air. This is especially true in the convective regions where the atmosphere is marginally stable, and where humidity increases of a few percent give sufficient energy to allow the boundary-layer air to support deep convection. Therefore, large-scale motions can suppress relative humidity to quite low values in regions of large low-level divergence, but they cannot increase the relative humidity in regions of convergence because of the efficient removal of moisture by convection in those regions. This asymmetry in the response of relative humidity to the large-scale circulation accounts for its potential to influence tropical SST in an important way.

Since in our simple model we are not explicitly solving for temperature profiles or convective processes, we must incorporate this asymmetry in a very crude way. We assume that condensation prevents the relative humidity from exceeding a critical threshold value of less than 100%. We choose a critical value of 86% for the relative humidity because, as described above, for the case of no large-scale motion, it produces a realistic climatology in our model. Although the value of the critical relative humidity is chosen for convenience rather than for more fundamental reasons, we believe that the asymmetry produced by this “relative humidity clipping” represents a real and important process that operates in the atmosphere. Our simple model allows us to illustrate this process and its role in coupling mean SST and SST gradients with the intensity of large-scale circulations.

Figure 4 shows how the zonal mean, the maximum, and the minimum temperatures vary as the magnitude of  $D$  is increased. For small values of  $D$  the model responds as expected: the mean temperature is unaffected by the sinusoidal forcing but the maximum and minimum diverge. For larger values of  $D$  the mean temperature begins to decline faster than the difference between the mean and the maximum temperature, so that the maximum temperature also decreases with increasing  $D$ . The mean temperature begins to decline when the divergence associated with the large-scale circulation becomes large enough to drive the relative humidity below its prescribed maximum value. The divergence of the low-level flow draws dry air into the boundary layer from above, which drives down the relative humidity. The effect of this localized drying of

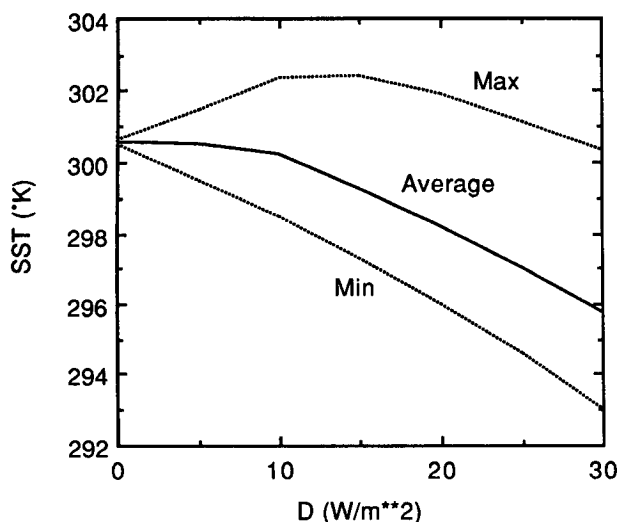


FIG. 4. Solutions for the mean (solid curve) and maximum and minimum (dashed curves) SST as functions of the east-west oceanic heat transport forcing parameter  $D$  in (14).

the boundary layer influences the SST over a large region as the dried air is advected away.

Some features of the model solution are shown in Fig. 5. The temperature distribution is peaked at the highest temperature and has a flat minimum. This is the opposite of the observed tropical oceans, where a large, relatively uniform warm pool occurs, but in the real oceans the ocean transport is very asymmetric with narrow and intense cooling at the eastern boundaries. The evaporative cooling peaks slightly upstream of the maximum temperature, because the relative humidity is suppressed upstream by the large-scale subsidence in the region of wind divergence. Zonal advection displaces the humidity minimum downstream of the region of wind divergence. The relative humidity maximum, cropped by the 86% lid, is similarly displaced downstream to coincide with the wind minimum, rather than the convergence maximum.

One would think that the length scale over which the dried air could influence the rest of the atmosphere would be limited to the distance the air could travel before being moistened by surface evaporation. This length scale is given approximately by

$$L_q = U\tau_d = 8 \text{ m s}^{-1} \times 2.5 \text{ days} \approx 1700 \text{ km}. \quad (15)$$

The scale of the region influenced by boundary-layer drying in the model is much larger than this estimate, however, because the advection of this dry air to adjacent regions cools the SST in those regions. The saturation humidity to which the air is relaxed by turbulent moisture exchanges is less in these regions of reduced SST, and the downstream advection of the lowered humidity spreads the cooling effect of localized divergence beyond the length scale given by (14). To illustrate this consider an oceanic heat transport that

consists of a half sine wave over a small fraction of the domain and a uniform compensating heating over the remainder of the domain:

$$\Delta F_0 = \begin{cases} D \sin\left(\frac{\pi x}{\alpha}\right) - A_0, & 0 < x < \alpha \\ -A_0, & \alpha < x < 1; \end{cases} \quad (16)$$

$A_0$  is a constant chosen to make the area-integrated oceanic heat flux divergence zero:

$$\int_0^1 \Delta F_0 dx = 0. \quad (17)$$

This structure might represent cooling by upwelling in a narrow region at one edge of the ocean basin, and weak heating in the remainder of the basin.

The solutions for the SST as a function of  $x$  for three values of the zonal-mean wind ( $u_0$ ) and with the oceanic transport given by (15) with  $D = 15 \text{ W m}^{-2}$  and  $\alpha = 0.15$  are shown in Fig. 6. The depressed SST extends about 3500 km downstream of the regions where the ocean currents are removing heat,  $0 < x/d$

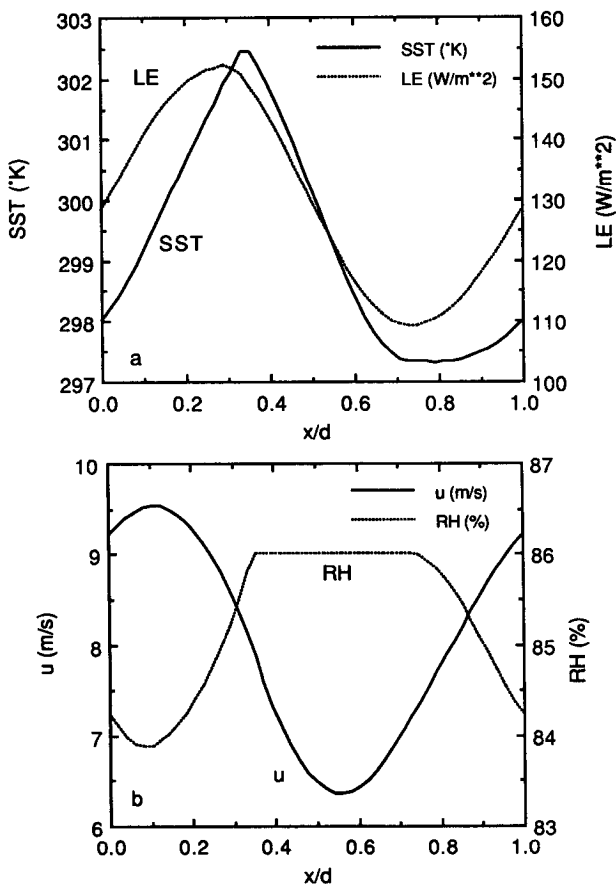


FIG. 5. Longitudinal dependence of the solutions for (a) SST, and evaporative cooling ( $LE$ ), and (b) zonal wind ( $u$ ) and relative humidity ( $RH$ ) for steady sinusoidal forcing with  $D = 15 \text{ W m}^{-2}$ .

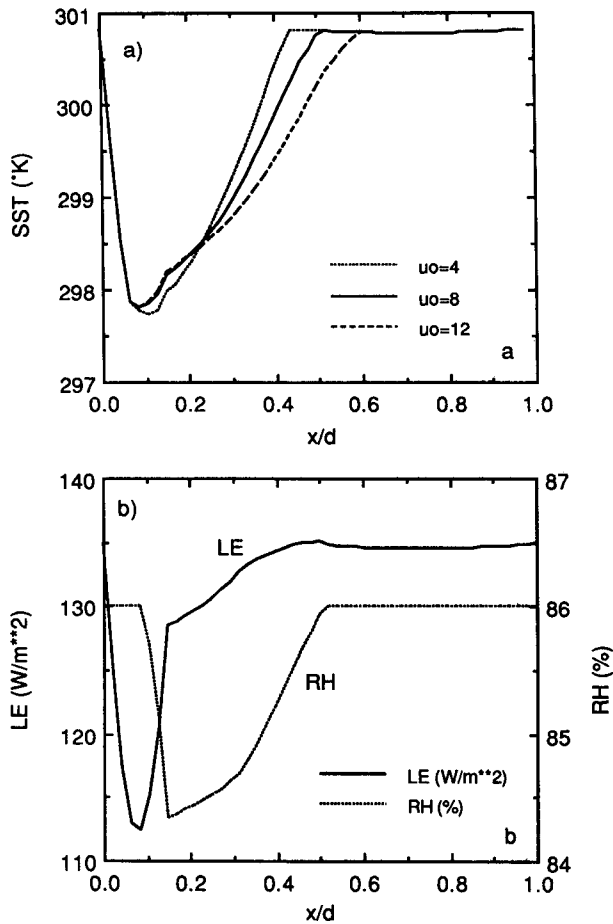


FIG. 6. (a) SST (in K) as a function of  $x$  for ocean transport as specified by (14) with  $D = 15 \text{ W m}^{-2}$  and  $\alpha = 0.15$ , so that a half sine wave cooling is applied between  $0 < x < 0.15$  and compensating warming elsewhere. The cooling effect is spread downstream by the zonal advection of a humidity deficit in the atmospheric boundary layer. Solutions for three values of the mean zonal wind speed are given:  $u_0 = 4, 8, \text{ and } 12 \text{ m s}^{-1}$ . (b)  $x$  dependence of the solution for evaporative cooling and relative humidity for the case of  $u_0 = 8 \text{ m s}^{-1}$  shown in (a).

$< 0.15$ , to  $x/d \approx 0.5$ . The domain of influence is not strongly sensitive to the mean zonal velocity. Beyond this region the SST is relatively constant and close to the value to which it converges in the absence of large-scale circulation effects. The size of the constant SST zone shrinks as the magnitude of the forcing increases, since the model is not linear.

The evaporative cooling is reduced in the region of coldest temperatures because of the dependence of saturation humidity on temperature. In the cold SST wedge downstream of the "upwelling" zone, the effect of the cold temperatures on vapor pressure and in turn the evaporation rate is nearly compensated by the effect of lowered relative humidities (Fig. 6b). Near the downstream edge of the cold wedge the evaporation actually reaches a weak maximum, because the effect

of suppressed relative humidity exceeds the effect of suppressed temperature.

One can consider the influence of a cloud shortwave feedback that changes the distribution, but not the area-averaged value of the insolation:

$$SW = SW_0 + \gamma(T_s - \overline{T_s}). \quad (18)$$

The overbar in (18) represents an area average, so that the area average of solar heating does not depend on the SST. Inclusion of such a feedback in our model has the same effect as decreasing the forcing of the SST gradient [decreasing the parameter  $D$  in (14) or (16)]. From Fig. 4 we can infer that the effect of a negative  $\gamma$  in (18) would be to decrease the SST contrast, but increase its mean value. Thus, we infer that the cloud shortwave feedback will *increase* the mean temperature. This behavior is a reflection of the important role of large-scale circulation in increasing the evaporation by ventilating the boundary layer. The model is of course very simple, and critical processes that are very complex in reality are represented with crude parameterizations. It is intended only to illustrate the important role of large-scale circulations in determining evaporation, convection, SST gradients, and mean SST in the tropics.

#### 4. Observations from the TAO array

In this section we present some observations that we believe show behavior like that of our simple model. These observations were taken from moored buoys on the equator that were deployed as part of the TOGA-TAO array for monitoring the state of the tropical Pacific (Hayes et al. 1991). These buoys provide ocean temperatures at the surface and at various depths down to 400 m, surface vector winds, humidity, and air temperature. The humidity and air temperature are taken at a height of about 3 meters above the surface. The humidity package is relatively new and has not been fully calibrated in the field, but errors are believed to be less than 5%. We will emphasize the relative changes in humidity rather than the absolute values. A small fraction of the TAO buoys are equipped with working humidity sensors, and, based upon the records that we have examined, these sensors tend to operate successfully for less than a year before requiring replacement. In Fig. 7 the daily mean SST and relative humidity measurements from buoys at two equatorial stations at  $170^\circ\text{E}$  and  $170^\circ\text{W}$  are shown as functions of time in 1992. Beginning at about day 150 (1 June 1992) the temperature at  $170^\circ\text{W}$  began to fall while that at  $170^\circ\text{E}$  began to rise. Simultaneously the relative humidity at both locations began to fall from values in the low 80s at both stations to values in the mid-70s at  $170^\circ\text{W}$  and low 70s at  $170^\circ\text{E}$ . The low humidities at  $170^\circ\text{E}$  continued until the sensor failed at about day 275. They persisted at  $170^\circ\text{W}$  until about December, when they rose back up to the low 80s again. The return

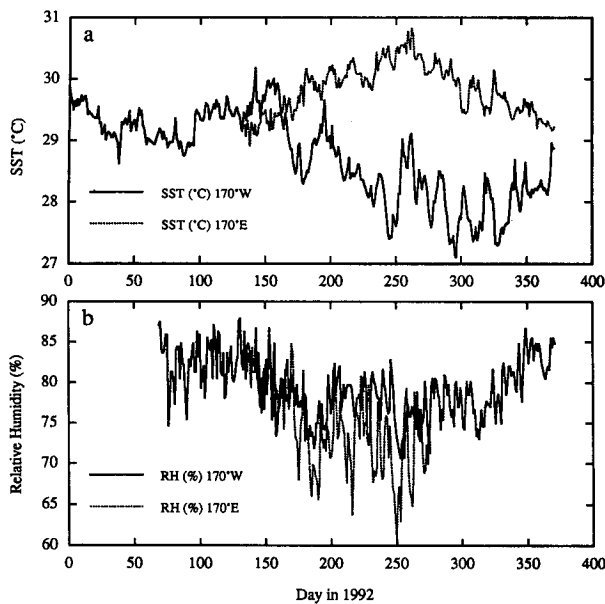


FIG. 7. Daily average TOGA-TAO array buoy measurements of (a) SST ( $^{\circ}\text{C}$ ) and (b) relative humidity (%) from buoys at  $0^{\circ}\text{N}$ ,  $170^{\circ}\text{W}$  (solid) and  $0^{\circ}\text{N}$ ,  $170^{\circ}\text{E}$  (dashed) plotted versus the day in 1992.

to higher relative humidity is associated with warming in the central Pacific and a concomitant retreat of the SST gradient toward the east. Also near the end of 1992 the easterly winds that peaked at about  $5\text{ m s}^{-1}$  at the date line began to decline rapidly (not shown). At the end of 1992 the warmest SST region was centered on the date line, and so forced a convergence anomaly there.

The distribution of SST and convection along the equator during this period can be seen in Fig. 8. At the beginning of the relative humidity record in March and April, the buoy at  $170^{\circ}\text{W}$  is located within the region of highest SST and greatest convection in the equatorial Pacific. Although the large-scale flow is probably converging moisture at this location, the convection keeps the averaged relative humidity between 80% and 85%. The transition that gave rise to the strong westward SST gradient between  $170^{\circ}\text{W}$  and  $170^{\circ}\text{E}$  around day 150 is associated with the combination of the end of the 1991–92 warm event and the normal seasonal transition from warm to cold SST in the eastern Pacific that occurs between the warmest month of April and the coldest month of October. During this transition the convection retreated to the west while a strong westward SST gradient developed in the central Pacific (Fig. 8). The association of a strong zonal SST gradient and advection from cold to warmer SST regions with lowered relative humidity in the boundary layer is consistent with the behavior of our simple model. It is likely that large-scale advective effects are responsible for the drying of the boundary layer, since

reductions in relative humidity occur simultaneously at two locations separated by 2000 km, and the largest reduction in relative humidity occurred at the warmer and more westward of the two sites. Even larger reductions of relative humidity with a similar time history were recorded at a buoy at  $2^{\circ}\text{S}$ ,  $165^{\circ}\text{E}$  (not shown).

## 5. Summary and conclusions

The sensitivity of tropical SST depends critically on large-scale, mesoscale, and boundary-layer processes that interact in complex and poorly understood ways. These scales also interact with the microphysical and radiative properties of clouds. Evaporative cooling is a very important term in the surface energy balance of the tropical oceans. Evaporation is very sensitive to SST and relative humidity in the boundary layer. If the relative humidity is assumed to remain constant during a climate change, then the rate of change of evaporative cooling with temperature is sufficient to give a very stable SST, even in the presence of substantial positive feedback from the greenhouse effect of water vapor. If the relative humidity does not change systematically with temperature, then evaporative cooling, through its sensitivity to SST, could provide the basic mechanism for making tropical SST stable over geologic time.

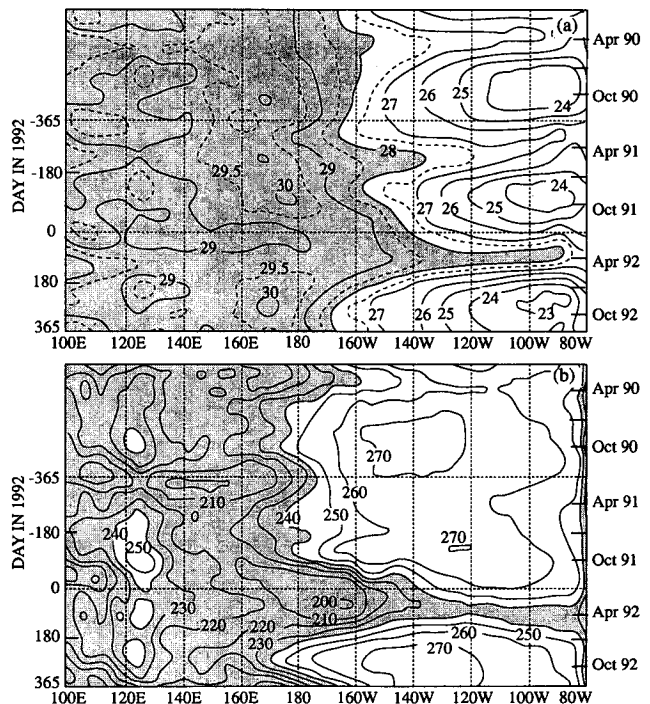


FIG. 8. Longitude time contour plots of monthly averaged (a) SST ( $^{\circ}\text{C}$ ) SST values greater than  $28^{\circ}\text{C}$  are shaded. (b) Outgoing longwave radiation ( $\text{W m}^{-2}$ ) averaged over the latitude belt from  $5^{\circ}\text{S}$  to  $5^{\circ}\text{N}$ . Shading indicates OLR values less than  $240\text{ W m}^{-2}$ . These figures were adapted from the December 1992 issue of the Climate Diagnostics Bulletin (CAC 1992).

Analysis of radiation budget data in relation to SST and large-scale circulation indices suggests that local enhancements of tropical convection are tightly connected with large-scale circulation patterns and SST gradients. This is consistent with the fact that large-scale moisture convergence is necessary to sustain the intensity of convection observed in the most active regions of the tropics. When SST and cloud forcing changes between warm and cold years in the tropical Pacific are averaged over the areas occupied by the large-scale circulation features associated with deep convection in the tropics, no evidence of a significant sensitivity of cloud forcing to SST can be found. In particular, sensitivity estimates based on spatial averages do not support a major role for shortwave cloud forcing in stabilizing tropical SST. For the changes that occurred in association with the 1987 El Niño, cloud albedo increases over the warmed water were compensated by cloud albedo decreases in adjacent warm SST regions where large-scale subsidence suppressed cloudiness.

Because shortwave cloud forcing is large and negative in regions of warmest SST in the tropics, it may act to reduce SST gradients, but large-scale circulations also respond sensitively to SST gradients. Large-scale circulations can influence evaporative cooling through their effect in ventilating the planetary boundary layer. Large-scale divergence and convergence have a net drying effect on the planetary boundary layer because mesoscale convective processes effectively dry the boundary layer in regions of large-scale convergence, whereas in regions of large-scale divergence only enhanced evaporation can moisten the boundary layer. Because the large-scale circulations respond sensitively to SST gradients, a large SST gradient will result in more efficient ventilation of the boundary layer by large-scale motions and a net increase in the average evaporation rate. A simple model is used to show possible relationships among SST gradients, large-scale circulations, evaporative cooling, and mean SST in the tropics. The asymmetry between the role of convergence and divergence on boundary-layer humidity is enforced by requiring that the relative humidity in the boundary layer not exceed a fixed critical value. If large SST gradients are forced by oceanic transport (e.g., upwelling at the eastern boundary), a large-scale circulation develops. The added ventilation of the atmospheric boundary layer provided by this large-scale circulation increases the evaporation and leads to cooling of the average tropical SST. Viewed in this context, the effect of shortwave cloud forcing in reducing SST gradients may actually work to increase the mean SST of the tropics.

A more complete model would recognize the joint response of evaporative cooling and shortwave cloud forcing to mean SST and SST gradients. In practice, important compensation undoubtedly occurs between changes in surface insolation and surface evaporation

that reduced the variability in the surface energy balance. Where convective clouds are present the insolation is reduced by enhanced cloud reflection, but in adjacent clear areas the evaporation is increased by entrainment of dry air through the top of the boundary layer, so that the net change in the surface energy balance between convective areas and cloud-free areas of large-scale divergence is relatively small. Data from ERBE and the TAO array suggest that the changes of insolation and evaporation are of comparable magnitude. ERBE indicates a change in absorbed solar radiation of about  $75 \text{ W m}^{-2}$  between convective and trade-wind regions (Figs. 2 and 3). Using the scaling presented in this paper (7), a change of boundary-layer relative humidity from 85% to 75% (Fig. 7) would cause a comparable change in the evaporative cooling of about  $80 \text{ W m}^{-2}$ . A more integrated understanding of the interactions among cloud radiative forcing, surface turbulent fluxes, convective processes, and large-scale dynamics is needed.

*Acknowledgments.* The first author benefited from conversations about this topic with J. Coakley, R. A. Houze, V. Ramanathan, E. Sarachik, K. Trenberth, J. M. Wallace, and P. J. Webster. J. Kiehl performed some calculations with his high-resolution radiative transfer model to give us added confidence in our calculations. Chidong Zhang suggested the use of the TAO data in this context. Vernon Kousky of the Climate Analysis Center kindly provided the data in Fig. 8. The editorial assistance of G. C. Gudmundson and the graphics work of Kay Dewar are appreciated. This work was supported by the Climate Dynamics Program, Atmospheric Sciences Division of the National Science Foundation under Grant ATM-90-06123 and the Earth Radiation Budget Experiment of the National Aeronautic and Space Administration under Contract NAS1-18153.

#### REFERENCES

- Arya, S. P., 1988: *Introduction to Micrometeorology*. Academic Press, 307 pp.
- Barkstrom, B. R., 1984: The earth radiation budget experiment (ERBE). *Bull. Amer. Meteor. Soc.*, **65**, 1170–1185.
- CAC, 1992: *Climate Diagnostics Bulletin*. 92/12. [Available from Climate Analysis Center, National Oceanic and Atmospheric Administration, 5200 Auth Road, Washington, D.C., 20233.]
- Charlson, R. J., J. E. Lovelock, M. O. Andreae, and S. G. Warren, 1987: Atmospheric sulfur: Geophysiology and climate. *Nature*, **326**, 655–661.
- CLIMAP, 1981: *Seasonal Reconstruction of the Earth's Surface at the Last Glacial Maximum*. Map and Chart Series, Geological Society of America. **36**.
- Cornejo-Garrido, A. G., and P. H. Stone, 1977: On the heat balance of the Walker circulation. *J. Atmos. Sci.*, **34**, 1155–1162.
- Ellingson, R. G., J. Ellis, and S. Fels, 1991: The intercomparison of radiation codes used in climate models: Long wave results. *J. Geophys. Res.*, **96**, 8929–8953.
- Fitzjarrald, D. R., and M. Garstang, 1981: Vertical structure of the tropical boundary layer. *Mon. Wea. Rev.*, **109**, 1512–1526.
- Fu, R., A. D. Del Genio, W. B. Rossow, and W. T. Liu, 1992: Cirrus-cloud thermostat for tropical sea surface temperatures tested using satellite data. *Nature*, **358**, 394–397.

- Hallberg, R., and A. K. Inamdar, 1993: Observations of seasonal variations in atmospheric greenhouse trapping and its enhancement at high sea surface temperature. *J. Climate*, **6**, 920–931.
- Hansen, J., A. Lacis, D. Rind, G. Russell, P. Stone, I. Fung, J. Lerner, and R. Ruedy, 1984: Climate sensitivity: Analysis of feedback mechanisms. *Climate Processes and Climate Sensitivity*. J. E. Hansen and T. Takahashi, Eds., AGU, **29**, 130–163.
- Hansen, J. E., I. Fung, A. Lacis, D. Rind, S. Lebedeff, R. Ruedy, G. Russell, and P. Stone, 1988: Global climate changes as forecast by Goddard Institute of Space Studies three-dimensional model. *J. Geophys. Res.*, **93**, 9341–9364.
- Hayes, S. P., L. J. Mangum, J. Picaut, A. Sumi, and K. Takeuchi, 1991: TOGA-TAO: A moored array for real-time measurements in the tropical Pacific Ocean. *Bull. Amer. Meteor. Soc.*, **72**, 339–347.
- Holton, J. R., 1992: *An Introduction to Dynamic Meteorology*, Third Ed., Academic Press, 511 pp.
- Houze, Jr., R. A., and A. K. Betts, 1981: Convection in GATE. *Rev. Geophys. Space Phys.*, **19**, 541–576.
- Lindzen, R. S., and S. Nigam, 1987: On the role of sea surface temperature gradients in forcing low-level winds and convergence in the tropics. *J. Atmos. Sci.*, **44**, 2418–2436.
- Manabe, S., and R. T. Wetherald, 1967: Thermal equilibrium of the atmosphere with a given distribution of relative humidity. *J. Atmos. Sci.*, **24**, 241–259.
- , and —, 1980: On the distribution of climate change resulting from an increase in CO<sub>2</sub> content in the atmosphere. *J. Atmos. Sci.*, **37**, 99–118.
- , and A. J. Broccoli, 1985: A comparison of climate model sensitivity with data from the last glacial maximum. *J. Atmos. Sci.*, **42**, 2643–2651.
- Mitchell, J. F. B., C. A. Senior, and W. J. Ingram, 1989: CO<sub>2</sub> and climate: A missing feedback? *Nature*, **341**, 132–134.
- Oberhüber, J. M., 1988: *An Atlas Based on the COADS Data Set: The Budgets of Heat, Buoyancy and Turbulent Kinetic Energy at the Surface of the Global Ocean*. Max-Planck-Institut für Meteorologie, No. 15, 19 pp.
- Ramanathan, V., 1981: The role of ocean-atmosphere interactions in the CO<sub>2</sub> climate problem. *J. Atmos. Sci.*, **38**, 918–930.
- , and W. Collins, 1991: Thermodynamic regulation of ocean warming by cirrus clouds deduced from the 1987 El Niño. *Nature*, **351**, 27–32.
- , R. D. Cess, E. F. Harrison, P. Minnis, B. R. Barkstrom, E. Ahmad, and D. L. Hartmann, 1989: Cloud-radiative forcing and climate: Results from the Earth Radiation Budget Experiment. *Science*, **243**, 57–63.
- Randall, D., R. D. Cess, J. P. Blanchet, et al., 1992: Intercomparison and interpretation of surface energy fluxes in atmospheric general circulation models. *J. Geophys. Res.*, **97**, 3711–3724.
- Raval, A., and V. Ramanathan, 1989: Observational determination of the greenhouse effect. *Nature*, **342**, 758–761.
- Reynolds, R. W., 1988: A real-time global sea surface temperature analysis. *J. Climate*, **1**, 75–86.
- Rind, D., and D. Peteet, 1985: Terrestrial conditions at the last glacial maximum and CLIMAP sea-surface temperature estimates: Are they consistent? *Quat. Res.*, **24**, 1–22.
- Roberts, R. E., J. E. A. Selby, and L. M. Biberman, 1976: Infrared continuum absorption by atmospheric water vapor in the 8–12 μm window. *Appl. Opt.*, **15**, 2085.
- Roeckner, E., U. Schlese, J. Biercamp, and P. Loewe, 1987: Cloud optical depth feedback and climate modeling. *Nature*, **329**, 138–140.
- Sarachik, E. S., 1978: Tropical sea-surface temperature: An interactive one-dimensional atmosphere ocean model. *Dyn. Atmos. Oceans*, **2**, 455–469.
- Sellers, W. D., 1965: *Physical Climatology*. University of Chicago Press, 272 pp.
- Somerville, R., and L. A. Remer, 1984: Cloud optical thickness feedbacks and the CO<sub>2</sub> climate problems. *J. Geophys. Res.*, **89**, 9668–9672.
- Stephens, G. L., and T. J. Greenwald, 1991: The earth's radiation budget and its relation to atmospheric hydrology. 1. Observations of the clear sky greenhouse effect. *J. Geophys. Res.*, **96**, 15 311–15 324.
- Wallace, J. M., 1992: Effect of deep convection on the regulation of tropical sea surface temperature. *Nature*, **357**, 230–231.
- Washington, W. M., and G. A. Meehl, 1984: Seasonal cycle experiments on the climate sensitivity due to a doubling of CO<sub>2</sub> with an atmospheric general circulation model coupled to a simple mixed-layer ocean model. *J. Geophys. Res.*, **89**, 9475–9503.
- Wiscombe, W. J., and J. W. Evans, 1977: Exponential-sum fitting of radiative transmission functions. *J. Comp. Phys.*, **24**, 416–444.